

## Modified Johnson Model for Permeability Estimation in Oil Well Cement During Early Hydration

<sup>1</sup>Syahrir Ridha, <sup>1</sup>Sonny Irawan, <sup>2</sup>Bambang Ariwahjoedi, <sup>3</sup>Khairun Azizi Bt. Mohd. Azizli,

<sup>3</sup>Muhd Fadhil Nuruddin and <sup>1</sup>Hilfan Khairy

<sup>1</sup>Faculty of Geosciences and Petroleum Engineering,

<sup>2</sup>Faculty of Science and Information Technology, Universiti Teknologi PETRONAS, Malaysia

<sup>3</sup>Faculty of Engineering, Universiti Teknologi PETRONAS, Malaysia

**Abstract:** Permeability is believed to be one of the major factors contributing to the fluid infiltration. Failure to control this property, especially during early hydration, may lead to secondary cementing operation that requires additional cost or in worst case may damage the well. Some models have been successfully applied in relating the cement permeability to its porosity. However, this models rather impractical for field use since measured porosity must be established first. In this study, the measured electrical conductivity was used as a tool to extract permeability of Class G oil well cement at elevated pressure up to 3000 psi and temperature up to 65°C during the first 24 h of hydration. The relationship between permeability and normalized conductivity follows power law correlation. Neither the Katz-Thompson equation nor Johnson equation differs much from the measured result, but the latter is closer to the exact result. Better result was obtained once it is fitted to the measured permeability data which resulting the modified version of Johnson model. New modified model is satisfied to the measured permeability data generated from other cement samples.

**Keywords:** Electrical conductivity, elevated pressure and temperature, oil well cement, permeability estimation

### INTRODUCTION

Oil well cement plays an important role to seal-off the casing and isolate the formation layers from fluids infiltration that might cause wellbore damage. Careful evaluation of cement after displacement is crucial to secure long-term durability. Therefore, construction of oil wells must effectively consider the cementing process involved to prevent fluids migration and to secure zonal isolation. The process for checking the cement after displacement are called cementing evaluation.

The application of cementing evaluation is currently focused only on detecting the quality of bond between the casing and the cement placed in the wellbore annulus between casing and wellbore. It is executed by using the sonic and acoustic log measurement. However, this technique has limitation to be used in evaluating the cement's physical properties development due to its density based principle (Vo-Thanh, 1991).

Promising technique using electrical impedance to evaluate cement's microstructural properties, including permeability, has been successfully applied (Nettelblad *et al.*, 1995; Christensen *et al.*, 1996; Shane, 2000; Zhang, 2008; Backe *et al.*, 2001; McCarter and Puyrigaud, 1995). The well known Katz-Thompson equation (Katz and Thompson, 1987) and Johnson equation (Johnson *et al.*,

1986) are most frequently discussed in the literature in relating permeability to conductivity as stated in Eq. (1) and (2):

$$k \approx c \cdot \frac{\sigma_b}{\sigma_o} d_{pore}^2 \text{ pore}(t) \quad (1)$$

where,  $k$  is permeability ( $\mu\text{m}^2$ ),  $c$  is a constant equal to 1/226 and  $\sigma_b/\sigma_o$  is normalized conductivity and  $d_{pore}$  is critical pore diameter:

$$k \approx \frac{\Lambda^2}{8/\sigma_{normalized}} \quad (2)$$

where,  $k$  is permeability ( $\text{m}^2$ ),  $\Lambda$  is a weighted pore volume-to-surface ratio that provides a measure of the dynamically connected part of the pore region.

These equations were empirically generated from rock samples and may not be fully applicable for cement due to the more rigid system. Since these samples were measured at mature stage and are not identical (Christensen *et al.*, 1996; Shane, 2000), further investigations are needed to assure the usefulness of these equations to cement system especially when the influence of elevated pressure and temperature are considered.

---

**Corresponding Author:** Syahrir Ridha, Faculty of Geosciences and Petroleum Engineering, Universiti Teknologi PETRONAS, Malaysia

Table 1: Composition of class G HSR cement

Raw oxide	Wt (%)	Bogue phases*	Wt (%)
CaO	64.3	C <sub>3</sub> S (tricalcium silicate)	62.5
SiO <sub>2</sub>	21.2	C <sub>2</sub> S (dicalcium silicate)	9.3
Al <sub>2</sub> O <sub>3</sub>	3.8	C <sub>3</sub> A (tricalcium aluminate)	2
Fe <sub>2</sub> O <sub>3</sub>	4.76	C <sub>4</sub> AF (tetracalcium aluminoferrite)	14.5
SO <sub>3</sub> 2.61			
MgO2.3			
K <sub>2</sub> O0.32			
Na <sub>2</sub> O0.46			

\*: Cement chemistry notation; C: = CaO; S: SiO<sub>2</sub>; A: Al<sub>2</sub>O<sub>3</sub>; F: Fe<sub>2</sub>O<sub>3</sub>

Table 2: Measurement scenarios for conductivity measurement

Sample No.	w/c	Temp. (°C)	Pres. (psi)
1	0.3	25	14.7
2	0.3	40	1500
3	0.3	65	3000
4	0.4	25	14.7
5	0.4	40	1500
6	0.4	65	3000
7	0.5	25	14.7
8	0.5	40	1500
9	0.5	65	3000

## METHODOLOGY

**Experimental setup:** American Petroleum Institute (API) Class G High Sulphate Resistant cement with water to cement (w/c) ratio of 0.3, 0.4 and 0.5, respectively is used this study. The cement sample composition measured by XRF analysis is presented in Table 1.

Class G cement powder was mixed to fresh water followed the standard from API RP 10A (2002). It was performed in the cement mixer equipment at 4,000 rpm for 30 min and it continued at 12,000 rpm for another 35 min. Once the slurry has been prepared, it was immediately placed into a 1 inch diameter x 1 inch tall cylinder rubber jacket. Then the sample was weighed using a digital balance, the weight measurement was used as an input in the electrical conductivity measurement.

**Electrical conductivity measurement:** Electrical conductivity information was obtained using CoreTestSystem™ AutoLab from New England Research (NER). The frequency measurement was set from 1 Hz until 0.2 MHz in a logarithmic sweep. Totally there were 20 data points of frequencies for each execution stored. These measurements were performed repeatedly until the sample reached 24 h of hydration. The experimental conditions for this measurement are presented in Table 2.

The cement bulk conductivity ( $\sigma_b$ ) was calculated from the bulk resistivity in Nyquist plot after it has been normalized for geometry factor (k), according to equation below:

$$\sigma_t = k / R_b \quad (3)$$

where,  $k = l / A$  is the geometry factor and  $l$  is the length of the specimen (4 cm) and  $A$  is the surface area perpendicular to the direction of electrical current (5.06 cm<sup>2</sup>).

The pore fluid was obtained by extracting the cement sample at certain pressure using HPHT API Filter Press. Once removed, the pore fluid was collected directly in a glass flask for conductivity measurement. The pore fluid was collected at several points in time, to obtain about 5 mL and followed by sealing of the orifice using filter press. The pressure profile was generated by pumping Nitrogen gas (N<sub>2</sub>) until it reached the desired pressure. The conductivity measurement after fluid extraction was immediately performed using conductivity meter.

**Mercury intrusion porosimetry (MIP):** MIP was used to measure critical pore diameter that is ranging from few nanometers to several hundred micrometers. This corresponds to the pore diameter at the inflection point on a cumulative volume versus pressure diagram. It also used to quantify the porosity by the same principle which is based on the capillary law governing liquid penetration into small pores as functions of surface and interfacial liquid tensions, pore-throat size and shape and the wetting properties of sample.

For samples prior to and after set, hydration rates of slurry were ceased before commencing MIP measurement. It was done by applying a solvent exchange procedure by replacing water inside the cement samples (Zhang, 2008). Hydration was set to be ceased at 5, 10, 16 and 24 h, respectively for each sample. About 4-8 g of cement sample was rinsed in a 100 mL Acetone in the sealable container and shaken vigorously. After soaking in acetone, the samples are dried up in oven-drying method at 80°C for 24 h and it followed by MIP measurement.

A Pascal 240 and 440 high pressure porosimeter were used in this study. The pressurization system was used a reversible pump operating continuously, which permits a perfect control in increasing/decreasing the pressurization speed of about 54 and 108 psi/sec and hence the maximum pressure of 29,000 and 58,000 psi for Pascal 240 and 440 can be reached in about 9 min.

**Permeability measurement:** Permeability measurements were performed on samples using gas permeameter-coreval 30 (Vinci Technology™) based on an unsteady-state (transient) method. The pressure fall off technique was applied on cores placed in a core-holder under hydrostatic confining pressure. The down-stream end of the sample was conditioned to atmospheric pressure whilst the upstream pressure used was 200 psig. This method makes possible the calculation of slip-corrected (Klinkenberg) permeability and Klinkenberg slip factor during single transient test and is a relatively fast technique compared to the steady-state method (API RP 40, 1998). Helium gas was then passed through the core sample and the pressure difference between the inlet and outlet is the main parameter to determine the permeability.

Prior to permeability measurement, all the samples were treated to the same conditions as discussed in MIP

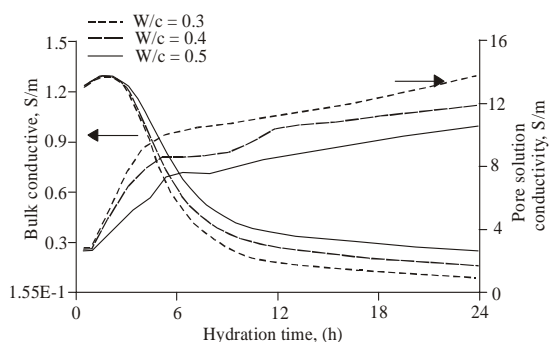


Fig. 1: Bulk and pore solution conductivity at atmospheric conditions as a function of hydration time

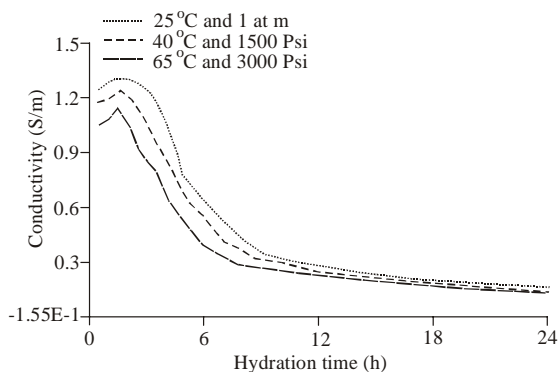


Fig. 2: Conductivity profile for w/c 0.4 mixture at elevated temperature and pressure

measurement. For samples at atmospheric condition, it was cured by placing the samples into 1x1 inch cylinder rubber jacket. Another sample conditioning was performed in the HPHT curing chamber which contained a sample cell with a dimension of 1x1x1 inch. Samples from the curing chamber were then directly cored into 1x1 inch cylinder core plugs. Three permeability measurements were made for each sample conditions to ensure data reproducibility and the final result was calculated by averaging these measurements.

## RESULTS AND DISCUSSION

**Electrical conductivity at early hydration:** A slight increase in bulk conductivity is observed at the beginning of hydration for all water cement ratio (Fig. 1). This is caused by the dissolution of ions of cement into the mixing water. However, as the hydration of cement progresses, the bulk conductivity decreases due to a combination of physical effects; one is the reducing volume fraction of solution and the other is increasing tortuosity of pore connecting path. At the similar period, an increasing trend is observed for pore solution conductivity which is attributed to the effect of ions movement dominated by  $\text{Ca}^{2+}$ ,  $\text{OH}^-$ ,  $\text{Na}^+$ ,  $\text{K}^+$  and  $\text{SO}_4^{2-}$ ,

respectively (Backe *et al.*, 2001). Values in the literature (Shane, 2000; McCarter and Puyrigaud, 1995) vary between 0.6 and 15 S/m, but the pore solution conductivity reported in this paper is relatively high, possibly due to the use of tap water instead of distilled water for cement mixing. The former is electrically more conductive due to the existence of additional active ions.

In this study, the conductivity for all samples at the different curing temperatures is corrected using Arps correlation (Ridha *et al.*, 2011; Arps, 1953). The conductivities of cement mixture with w/c 0.4 at specific curing temperature and pressure plotted as a function of hydration time is shown in Fig. 2. The trend of decreasing conductivity, as shown by three different conductivity profiles in the graph, is due to the effect of accelerated hydration which is accomplished by increasing the temperature and pressure. As such the pore pressure becomes lower when compared to similar period with normal curing condition.

**Permeability prediction based on the existing models:** Measured data of cement permeability at specific curing conditions is presented in Table 2. It can be seen that permeability is decreased as hydration proceed. Similar profile of decreasing permeability can be observed for samples at the same hydration period and water cement ratio as an effect of elevated curing temperature and pressure. This may be due to accelerated hydration experienced by the cement mixture as temperature increases and at the same time the pore size is narrowed due to the applied pressure.

In the Katz-Thompson model, the pore radius was measured using MIP measurement. As such, by knowing cement's pore radius and normalized conductivity, permeability of cement sample can be directly calculated. Similar principle is occurred to Johnson model; however the pore volume-to-surface ratio was computed from the particle expansion model (Ridha *et al.*, 2011). Completed results of MIP measurement are given in Table 3.

Figure 3 showed permeability result for both the models compared to the measured data. The models seem to predict a smooth, monotonic decrease in permeability due to a function of the normalized conductivity and microstructure parameters. Relatively after 6 h of hydration, the values of permeability calculated from the equations are higher than those obtained by the actual permeability tests. A higher gab seems to be existed once the hydration continues to proceed especially in the lower water cement ratio.

The effect of curing temperature and pressure on permeability evolution indicated that the more temperature and pressure applied, the more permeability will be decreased. However, at mature states, different result was revealed at which permeability increased as a function of temperature (Ludwig, 1959).

Table 3: Measured pore radius of class G cement from MIP measurement

w/c	T/P (°C/psi)	Pore radius ( $\mu\text{m}$ )				
		Hydration time (h)	5	10	16	24
0.3	25/14.7		8.92	7.42	6.53	4.71
0.3	40/1500		8.22	6.29	5.37	4.11
0.3	65/3000		7.63	5.86	4.27	2.75
0.4	25/14.7		12.38	10.73	8.82	6.97
0.4	40/1500		11.75	8.52	7.92	6.17
0.4	65/3000		10.64	8.96	6.82	4.75
0.5	25/14.7		15.58	13.31	11.28	9.87
0.5	40/1500		14.38	11.97	10.77	8.17
0.5	65/3000		13.82	10.72	9.27	7.22

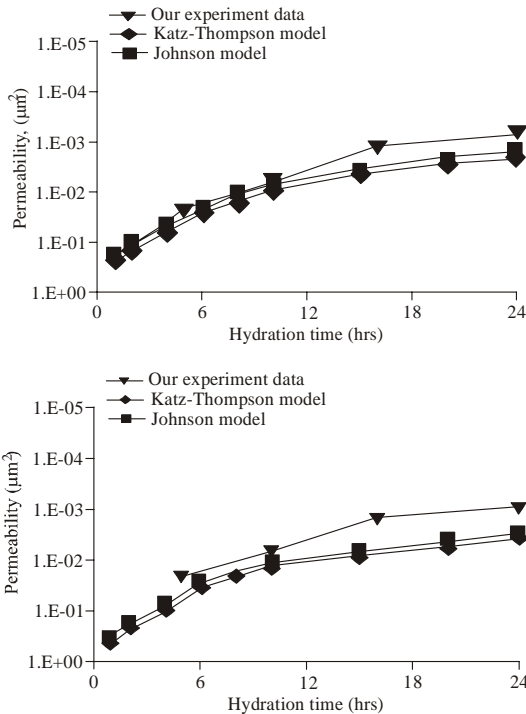


Fig. 3: Permeability data calculated from Katz-Thompson and Johnson equation compared to the measured data, (a) w/c = 0.4 at 40°C & 1500 psi, (b) w/c = 0.5 at 65°C and 3000 psi

**Modified model for permeability prediction:** It can be argued that the microstructural parameter in the Johnson model was less affected by the elevated temperature and pressure. This can be seen as the hydration was accelerated the pore volume to surface ratio was decrease slightly comparing to the normal curing condition. In the other hand, the pore radius parameter used in Katz-Thompson equation was relatively strong affected by the elevated curing condition (Fig. 4). As such, as also shown in Fig. 3, the Johnson model tends to have better prediction in comparing to the Katz-Thompson model.

The constant in Johnson model was modified as it considered being not fully appropriate in cement

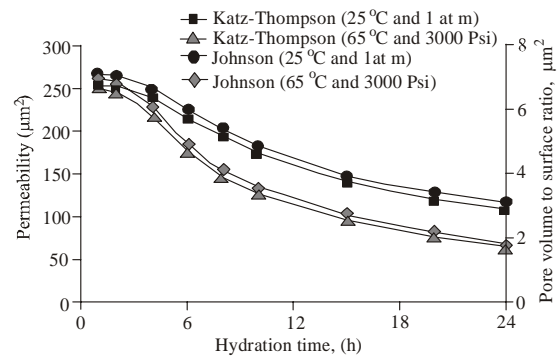


Fig. 4: Microstructural parameter development employed in the Katz-Thompson and Johnson equation as a function of hydration time with respect to different curing condition

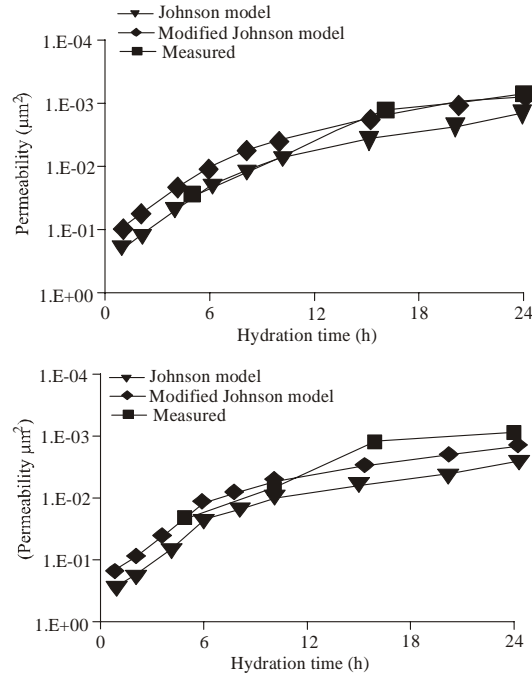


Fig. 5: Comparison of the measured and calculated of permeability using modified Johnson equation, (a) w/c = 0.4 at 40°C & 1500 psi, (b) w/c = 0.5 at 65°C and 3000 psi

application due to the characteristics changing of the pore shape with time and furthermore this pore structure is much more complicated than that of porous rocks. Modification was obtained by fitting the equation to the measured data of permeability. This is reasonably acceptable since the previous constant number was obtained from sedimentary rock samples which is physically has different structures compared to cement. The constant fitting parameters for Johnson model is 16 as mention in Eq. (4). Comparison of the experimental data after constant parameter fitting is well matched as given in Fig. 5.

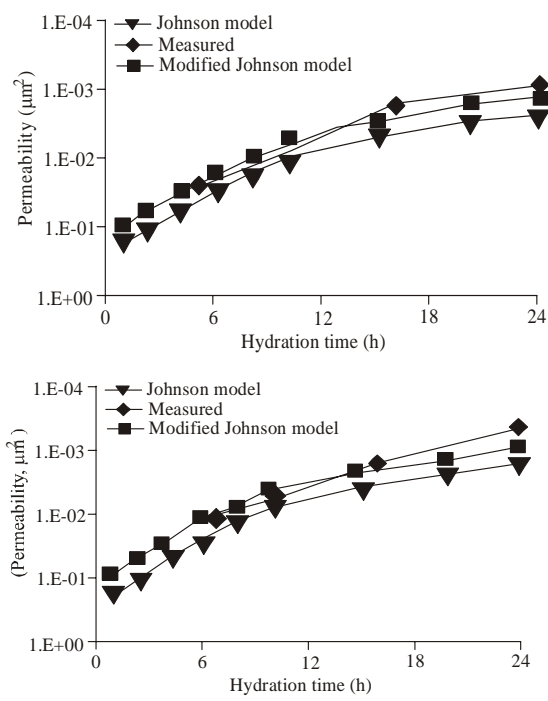


Fig. 6: Comparison of measured and calculated permeability on new cement samples, (a) w/c = 0.3 at 25°C and 1 atm, (b) w/c = 0.3 at 40°C and 1500 psi

$$k \approx \frac{\Lambda^2}{16/\sigma_{normalized}} \quad (4)$$

Verification was done for another cement samples at different water cement ratio and curing conditions within similar hydration period. A reasonably good comparison of permeability value between measured and calculated data of new cement sample confirms its applicability (Fig. 6).

## CONCLUSION

Measured permeability data of neat class-G cement during 24 h of hydration have been correlated to electrical conductivity in the form of Katz-Thompson and Johnson models. The effect of elevated temperature and pressure are carefully considered. Result found that none of models differs much from the measured data, but the Johnson model is closer to the exact result. Modified version of Johnson equation by fitting the constant parameter into the measured data is shown to be more applicable for permeability prediction. Increasing constant number in the new equation implied that the cement structure has more complex nature in term of microstructure properties. The permeability results at different curing conditions

estimated using the modified equation is compatible with experimental data. This modified equation may be used to predict cement permeability in the mature stage and as such can monitor the durability of well cement in place.

## ACKNOWLEDGMENT

The financial support from University Internal Research Funding (URIF) Universiti Teknologi PETRONAS is gratefully acknowledged.

## REFERENCES

- API RP 10A, 2002. Specification for Cements and Materials for Well Cementing. 23rd Edn., American Petroleum Institute.
- API RP 40, 1998. Recommended Practices for Core Analysis. 2nd Edn., American Petroleum Institute.
- Arps, J.J., 1953. The effect of temperature on the density and electrical resistivity of sodium chloride solutions. Trans. AIME, 198: 327.
- Backe, K.R., O.B. Lile and S.K. Lyomov, 2001. Characterizing curing cement slurries by electrical conductivity. SPE Paper 74694.
- Christensen, B.J., T.O. Mason and H.M. Jennings, 1996. Comparison of measured and calculated permeabilities for hardened cement pastes. Cement Concrete Res., 26(9): 1325-1334.
- Johnson, D.L., J. Koplik and L.M. Schwartz, 1986. New Pore-Size Parameter Characterizing Transport in Porous Media. Phys. Rev. Lett., 57: 2564-2567.
- Katz, A.J. and A.H. Thompson, 1987. Prediction of Rock Electrical Conductivity from Mercury Injection Measurements. J. Geophys. Res., 92(BL): 599-607.
- Ludwig, N.C., 1959. Chemistry of Portland Cement Used in Oil Wells. Oil-Well Cementing Practices in the United States. API Publisher, New York, pp: 27-33.
- McCarter, W.J. and P. Puyrigaud, 1995. Water Content Assessment of Fresh Concrete. Proceeding of the Institution of Civil Engineers-Structures and Buildings, 110(4): 417.
- Nettelblad, B., B. Ahlen, G.A. Niklasson and R.M. Holt, 1995. Approximate determination of surface conductivity in porous media. J. Phys. D. Appl. Phys., 28: 2037-2045.
- Ridha, S., S. Irawan and B. Ari wahjoedi, 2011. Microstructure Parameter Estimation in Permeability Calculation of Well Cement during Early Hydration by a Simple Particle Expansion Model. Proceeding of 3rd National Postgraduate Conference (NPC), University Technology PETRONAS, Sep. 19-20.
- Shane, J.D., 2000. Electrical conductivity and transport properties of cement based-materials measured by impedance spectroscopy. Ph.D. Thesis, Northwestern University.

- Vo-Thanh, D., 1991. Effects of fluid viscosity on shear-wave attenuation in partially saturated sandstone. *Geophysics*, 56(8): 1252-1258.
- Zhang, J., 2008. Microstructure study of cementitious materials using resistivity measurement. Ph.D. Thesis, the Hong Kong University of Science and Technology.